

## COMPARISON OF PASSIVE AND ACTIVE FIDUCIALS FOR OPTICAL TRACKING

J. Odmins<sup>1</sup>, K. Slics<sup>1</sup>, R. Fenuks<sup>2</sup>, E. Linina<sup>2\*</sup>, K. Osmanis<sup>1</sup>, I. Osmanis<sup>2</sup>

<sup>1</sup>Hansamatrix Innovations Ltd., 1 Ziedleju Str., Marupe, LV-2167, LATVIA

<sup>2</sup>LightSpace Technologies, 1 Ziedleju Str., Marupe, LV-2167, LATVIA

\*e-mail: elza.linina@lightspace3d.com

The paper analyses the constraints related to optical tracking of an HMD with a single commercial binocular stereoscopic optical tracking system and offers an overview of different factors affecting the best active fiducial set-up and marker geometries for reliable tracking with a focus on the rotational accuracy of a marker.

Two IR diode models with different emission characteristics were tested as active fiducials and the results were compared to localization accuracy of passive fiducials. In terms of preferable marker geometry, it was found that the area enclosed by the fiducials should be maximized. Thus, due to geometrical constraints, very small marker geometries may not be stable or feasible entirely. Rotational accuracy was analysed for cases when the marker was not directly facing the tracking device and it was found that rotation about one axis introduced errors to the determined orientation in space related to the other axes as well.

**Keywords:** Active fiducials, angular accuracy, marker geometry, optical tracking, passive fiducials.

### 1. INTRODUCTION

Augmented reality (AR) devices have been widely researched for the past few decades and are envisioned to penetrate all aspects of everyday life – starting with professional fields such as manufacturing and education, and most notably – the medical field [1]. Even though different implementations of AR already exist [2], the medical field is by far the most demanding in terms

of accuracy and comfort of use since surgical procedures can last for several hours. For example, the utilization of an AR headset as a vision aid during surgical procedures puts enormous pressure on the accuracy of image representation [3]. While optics and human perception play a major role in image quality [4], the other side that is equally important for achieving the desired image accu-

racy is object tracking. In this case, it is the tracking of a headset within the real-world space and in relation to the patient and surroundings. The image rendering engine has to rely on accurate position and orientation of the head-mounted display (HMD). Thus, tracking a headset pose accurately is as relevant as providing naturalistic visual cues.

Currently available AR headsets positioned as enterprise-level devices base their pose tracking on visual simultaneous localization and mapping (vSLAM) algorithms, which typically cannot provide the much-needed accuracy in medicine [5]. Depending on the type of task, the preferable image overlay (and consequently, pose tracking) accuracy has to be substantially better than 1 millimetre – although in some scenarios it might be acceptable to achieve lower accuracy [6]. Thus, one of the options is to complement vSLAM with other means of pose tracking or rely on a different tracking solution altogether [7].

One such approach is optical tracking of fiducial markers. This type of object localization within space has long been the go-to method for accurate pose estimation with full 6 degrees of freedom [8]. With the raising popularity of AR devices, research on the topic of pose estimation is still ongoing and many improvements have been made in the past decade [9]–[11]. Based on binocular stereoscopic cameras, commercial optical tool tracking solutions for medical (surgical) settings have been developed [12]. The claimed optical tracking accuracy for tool positioning, for example,

during minimally invasive procedures is on the order of 0.1 mm. Better accuracies have been demonstrated by multi-camera setups – for example, with trinocular configuration reaching 0.04 mm [13]. Nevertheless, these very high accuracy values are typically attributed to translation, while in visualization rotational accuracy is similarly important.

Optical tool tracking solutions are already being used in the medical field and many surgical rooms have already been equipped with some type of an optical tracking system. With AR displays offering unprecedented real-time data visualization and thus slowly penetrating the medical field, preinstalled optical tool tracking systems can be repurposed for dual use. The ability to track multiple markers simultaneously also enables the tracking of an HMD with high accuracy – higher than could be achieved by solely relying on vSLAM. Furthermore, utilization of a single tracking device for tools and headset naturally unites coordinate systems, thus alleviating the integration of AR visualizations in medical procedures.

The primary aim of the present research is to analyse the constraints related to optical tracking of an HMD with a single commercial binocular stereoscopic optical tracking system and to develop and verify active fiducial and marker configurations for reliable tracking (putting emphasis on maximizing effective angular range and rotational accuracy).

## 2. MATERIALS AND METHODS

---

It should be noted that AR HMDs come in different varieties, including both optically see-through (OST) as well as video see-through (VST) systems [14]. For medi-

cal applications OST displays can provide an additional level of safety; nevertheless, fully immersive VR headsets have also been successfully applied and shown as a

valuable addition to the medical professionals [15]. The main feature of a virtual or augmented stereoscopic display is that it provides a sense of 3D depth and thus – an additional layer of spatial awareness to the medical professionals.



*Fig. 1.* The multifocal HMD prototype system used for tracking experiments.

For the aim of this study, the previously developed prototype system (Fig. 1) is used – a multi-focal OST AR display [16], which provides the user with a 3D image and also matches vergence and accommodation cues, thus providing better eye comfort. While specific geometrical constraints are defined by the layout design of the particular device, general concepts are applicable universally.

Since commercially available AR HMDs were initially oriented towards a wider area of application, including consumer markets, the emphasis was put on ease of use and thus visual simultaneous localization and mapping (vSLAM) as a means of pose tracking. The advantage of vSLAM type tracking is that it can map any reasonably feature-rich environment and provide pose tracking based on the relative position of a headset in respect to the surroundings. Nevertheless, in certain situa-

tions the performance can be compromised and overall accuracy is on the order of millimetres. For applications where accuracy is extremely important, vSLAM can be substituted or complemented by depth data derived directly from time-of-flight cameras [17]. It has been shown that complementing a commercial headset with marker-based reference detected by the on-board sensor arrays, the accuracy of pose detection can be reduced to sub-millimetre values [18].

When an HMD system does not house a diverse set of sensors, other approaches have to be utilized. The target pose-tracking accuracies ideally have to be in the order of  $<0.05$  mm for translational motion and  $<0.05^\circ$  for the angular localization. Significant effort has been put towards reducing translational errors and the research commonly focuses on translational accuracy while omitting data on angular accuracy. However, for the case of HMD tracking (which means essentially tracking the position of a human head), translational motion is quite uncommon, a much more natural and often occurring motion is rotation. Thus, special attention has to be devoted to achieving accurate and stable tracking of angular changes.

One of the obvious solutions to surgical AR HMD tracking is the utilization of existing navigation systems that have been already adapted for tool tracking [19]. These are designed to visualize tool tips beyond their visibility within the human body during, for example, minimally invasive procedures. The precise localization of the tool tip is based on rigid and known geometry of the tool and a precisely defined optical marker comprised of several fiducials (typically 3–6 fiducials). Fiducials are tracked by a system of precisely intercalibrated stereoscopic cameras to derive essential coordinates of a fiducial within a 3D space, including the orientation.

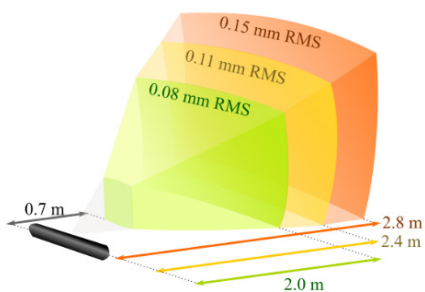


Fig. 2. Atracsys fusionTrack 500 accuracy (pose RMS) for different working distances.

Overall, it would be convenient to utilize a common optical tracking system for the simultaneous tracking of both the HMD and the surgical tools. Thus, this study focuses on marker development and performance evaluation of AR headset tracking using medical stereoscopic tool tracking system *Atracsys FusionTrack 500*.

The Atracsys fusionTrack 500 is a real-time optical pose-tracking system that can track markers in real-time video streams. The fusionTrack is composed of two cameras that observe fiducials simultaneously, and uses triangulation to calculate the locations of these fiducials with a measurement rate of 335 Hz [20].

Atracsys FusionTrack 500 specifications:

Resolution: 2.2 Mpix

Refresh rate: 335 Hz

Working distance: 0.7 to 2.8 m (Fig. 2)



Fig. 3. Comparison of reflectivity as detected by Atracsys FusionTrack 500 for passive fiducials: out of package (bottom row) and after extended handling (top row).

*Atracsys FusionTrack 500* and similar systems are designed to work with passive as well as active markers. The camera system is equipped with infrared emitters placed around both camera lenses that are intended for the illumination of retroreflective fiducials. Most commonly, retroreflective fiducials are either flat circles or three-dimensional spheres that are highly visible to the infrared cameras. Spherical fiducials are considered more versatile – as they can be observed from larger angles; nevertheless, for tool tracking flat fiducials perform equally well. Unfortunately, in the setting of surgery, passive markers are subject to contamination and loss of reflectivity (Fig. 3), which interferes with robust pose tracking. Generally, retroreflective fiducials are treated as consumables and changed during set time intervals or upon need.

An alternative to the retro-reflective spheres or disks is the use of active markers comprised of infrared (IR) light emitting diodes (LEDs) whereby a pattern of LEDs is arranged on a rigid structure associated with a tool or a headset. While this approach ensures a more robust overall tracking (mostly due to LEDs not being as prone to contamination as the large-surface passive markers), there are other challenges that often place IR LEDs at a disadvantageous position.

IR LEDs require electrical power to provide tracking capability, which means a battery or some other power-source needs to be associated with the active marker. For tool tracking, this adds to the weight and can make a tool more difficult to use. For a battery or accumulator-type power source, some monitoring is also necessary as it can be detrimental to the health of a patient if a procedure has to be stopped midway to change an empty battery.

For HMDs the use of active markers can be justified more easily as the additional

weight of LEDs is just a small fraction of the total weight of such a device; however, power consumption can still cause issues. Small form-factor LEDs can be driven with up to 100 mA of current, which adds up to about a 100 mW. A marker is typically comprised of 3 to 6 LEDs that can be a considerable number if the device is bat-

tery-powered. In tethered devices, power consumption might not be the primary concern; however, the dissipated heat is a prominent issue, as it can interfere with the comfort of wearing an HMD and can negatively affect the performance of embedded semiconductors such as microcontrollers, processors, FPGA chips, etc. [21].

### 3. RESULTS AND DISCUSSION

#### 3.1. Fiducial Analysis

*Atracsys FusionTrack 500* is designed to work well with different types of passive markers. For this purpose, retroreflective spheres (Navigation Markers produced by ILUMARK) of 12 mm in diameter were chosen as a reference for making comparisons between different active IR LED fiducials. Due to the limited resolution of the cameras, any fiducial needs to reach a certain size threshold reported by the camera sensor to be recognised as a fiducial. In the case of IR LEDs as active markers, the reported size is a function of both the driving current of an LED and the physical distance to it. With the default image acquisition and processing parameters, different LEDs (in terms of emitter size and

consumed power) were tested by varying the forward current, distance from the camera system, and tilt angle of LEDs with respect to the camera system. Additionally, the tracking jitter of a stationary fiducial in relation to its size (controlled by current) and distance was also determined.

Two IR LEDs from Osram – SFH 4250-S and SFH 4053 – were investigated and compared to the passive markers. The SFH 4250-S was endorsed by developers of the tracking system, while the SFH 4053 was chosen due to the relatively small package and high brightness. The main differences are due to the emitter size and emission angle. The key characteristics of both LEDs are shown in Table 1.

**Table 1.** Comparison of the Main Parameters for IR LEDs Produced by Osram – Models SFH 4250-S and SFH 4053

	SFH 4250-S	SFH 4053
Centroid wavelength, nm	850	850
Maximum forward current, mA	100	70
Emission half angle, °	60	70
Active chip area, mm <sup>2</sup>	0.3×0.3	0.2×0.2
Total radiant flux, mW	100	35
Radiant intensity, mW/sr (at I <sub>f</sub> max)	18–28	4.5–11.2
Package	PLCC-4 (3.65 mm×2.95 mm×2.15 mm)	0402 (1 mm ×0.5 mm×0.45 mm)

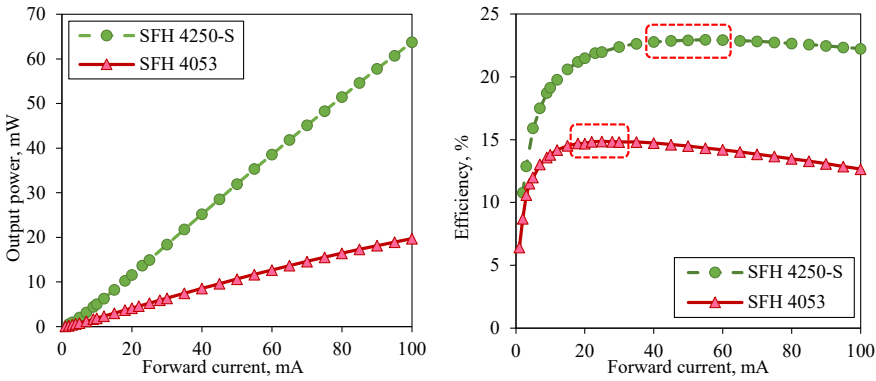


Fig. 4. **Left:** Output power of SFH 4250-S and SFH 4053 LEDs as a function of driving current. **Right:** Efficiency of SFH 4250-S and SFH 4053 LEDs as a function of driving current.

Due to the fact that electronic components often vary in bins and manufacturer datasheets are provided only for reference values, the actual optical output power and efficiency of both LEDs were determined (Fig. 4) experimentally.

The measurements were carried out using the *Agilent Technologies 3606A* power supply in constant current mode. The voltage values were read from the built-in voltmeter. The output power was measured

by *Thorlabs PM400* in conjunction with the *SI146C integrating sphere* sensor.

It can be noted that from the efficiency standpoint, the best performance from the SFH 4250-S LED can be expected for forward current in the range from about 40 mA to 60 mA, whereas for SFH 4053 the same is true for the 18 mA to 30 mA range. In terms of absolute efficiency, the SFH 4250-S is superior.

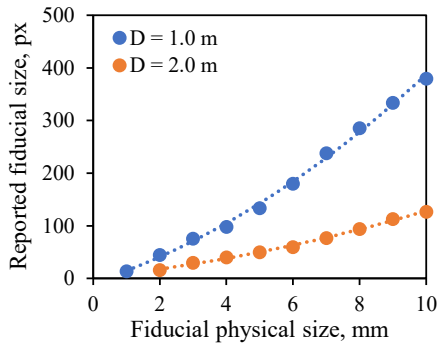


Fig. 5. Atracsys FusionTrack 500 reported fiducial size in pixels at physical distances of 1.0 and 2.0 m for different-sized passive flat disk markers.

A passive retroreflective fiducial forms a predictable response signal on the image capturing sensors of *FusionTrack 500* system – there is a direct correlation between the number of activated pixels and the physical size of the fiducial (Fig. 3).

However, for active LED-based fiducials this is not as straight forward – the reported size varies with both the distance (Fig. 6 (right)) and the forward current used to drive the LED (Fig. 6 (left)).

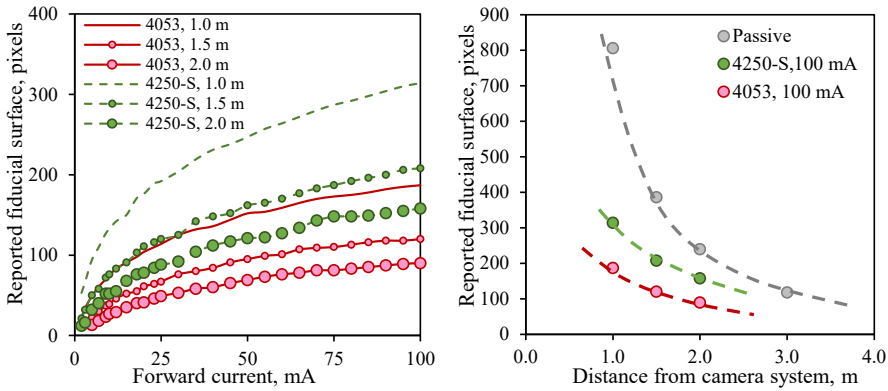


Fig. 6. **Left:** the reported fiducial surface area for SFH 4250-S and SFH 4053 LEDs at different distances and with different driving currents. **Right:** the reported fiducial size as a function of distance to the camera system at maximum driving current with passive marker data (ILUMARK, 12 mm) for reference.

For reliable detection, the activated area on the camera sensor has to be large enough to be recognised as fiducial. By default, it is set to 40 pixels. As it can be seen, the standard passive fiducial balls at relevant working distances of 1.5 m and 2.0 m result in a relatively large signal – approximately 400 pixels and 240 pixels, respectively. In contrast, the LEDs driven at maximum forward current for the same distances of 1.5 m and 2.0 m can achieve only almost half that – 200 and 160 pixels, respectively.

At this driving current of 100 mA, a single LED consumes almost 0.29 W and it would amount to at least 1.16 W total power consumption for a typical 4-fiducial

marker in continuous driving mode. A lot of this power is dissipated as heat, which can influence the performance of the LEDs themselves as well as be inconvenient to the user. The focus further is thus on the accuracy and consistency of detection for different driving currents (as related to the size detected by the cameras). For this purpose, different fiducials were rigidly fixed in relation to the tracking camera system and series of registration frames were accumulated alongside with complementary data about the registered coordinates of a fiducial. For LED markers, the relevant current range – between 20 and 100 mA – was analysed (Figs. 7 and 8).

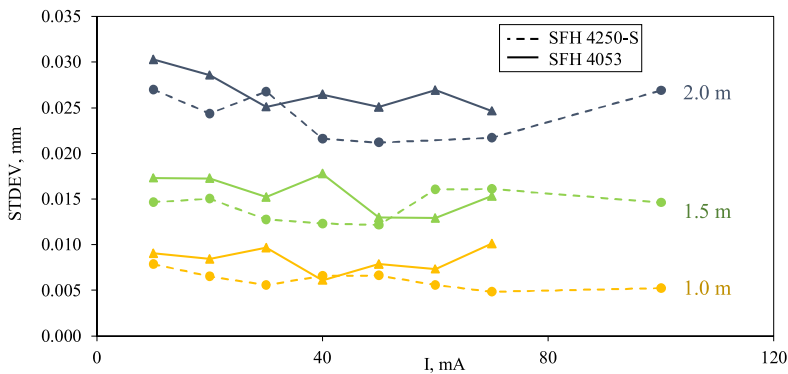


Fig. 7. Comparison of active fiducial (IR LEDs SFH 5042-S and SFH 4053) localization accuracy at different distances to the camera system for varying driving currents (20 mA to 70 mA and 20 mA to 100 mA, respectively).

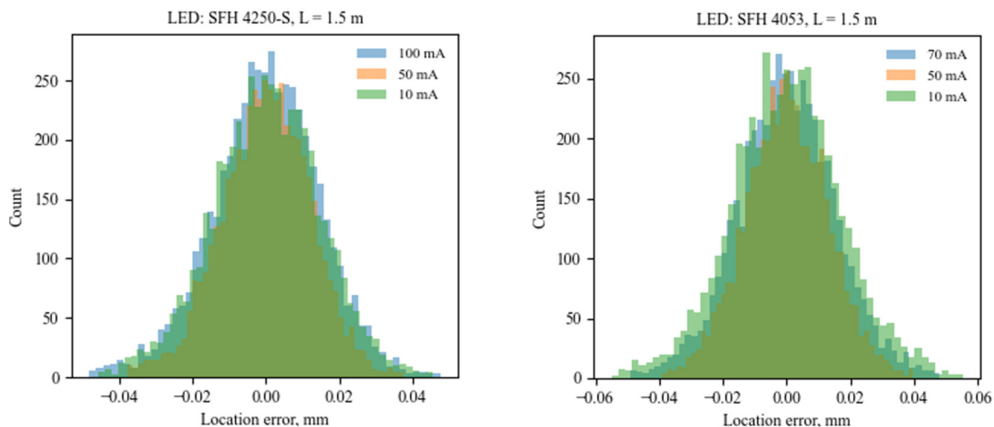


Fig. 8. **Left:** Distribution of the determined coordinate values around the mean for SFH 4250-S at 1.5 m distance from the camera-system (shown for 10, 50 and 100 mA driving current). **Right:** Distribution of the determined coordinate values around the mean for SFH 4053 at 1.5 m distance from the camera-system (shown for 10, 50 and 70 mA driving current). The FWHM of these distributions are shown in Fig. 7.

The registration error overall follows a normal distribution. It was found that, generally, when the fiducials are above the critical limit for detection, no distinct relation between the dispersion of data and the fiducial size (or rather, the current) could be found. On a small scale in consecutive time intervals during which the supposed ambi-

ent conditions – most notably vibrations – were at similar levels, some dependence on the size can be distinguished. These differences, however, are well below the claimed accuracy levels of the tracking system and essentially negligible. Thus, the use of smaller driving currents can easily be justified.

### 3.2. Marker Construction Analysis

A marker is a rigid array of multiple fiducials. To determine the orientation of a marker, it must be comprised of at least three non-aligned fiducials [22]. Generally, for best possible results, the designed geometry should not have any axes of symmetry and the distances between any two fiducials should be different.

For improved positional and rotational accuracy, markers are comprised of four fiducials instead of three. This helps reduce the pose data errors as they can result in a jittery image which is very unpleasant and distracting for the user even so far as to become unusable. An example of feasible marker geometry can be seen in Fig. 9.

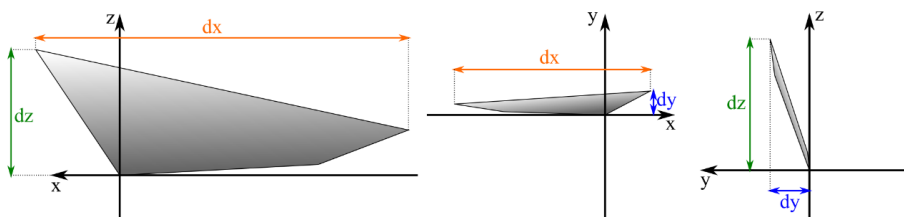


Fig. 9. Sample geometry of a four-fiducial marker. The fiducials are placed at the vertices and form a surface in 3D space.

In order to achieve the best tracking accuracy, the distance between the fiducials has to be large – small displacements of the head then translate into noticeable displacements of the marker fiducials. To achieve good angular resolution (and thus also minimize jitter), the area of the marker should also be maximized as discussed further.

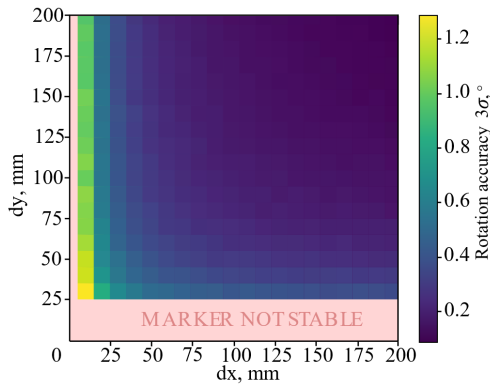


Fig. 10. Rotational accuracy as determined by 3 standard deviations about mean pose of markers with sides of different lengths.

Physically creating and testing different marker geometries is a very time-consuming process. Thus, to determine the best approach, synthetic data were generated and analysed with the *Atracsys Matlab Marker Analyzer*. This tool allows analysing marker geometries (checks segment lengths and symmetries), and can provide the user with expected marker accuracy

data. This is achieved by applying the typical noise to the true location of each fiducial and determining the resulting marker location and orientation as if it were detected by the cameras. This process is then repeated to obtain the expected standard deviations of marker location and orientations.

Figure 10 shows the rotational accuracy for markers of different sizes and aspect-ratios – the component is set to be 0 for all markers. Due to the fact that all segments between markers need to be of different lengths (the minimum difference needs to be at least 5 mm), some smaller geometries are not feasible at all or behave in an unstable manner – the rotational errors for markers with mm are well beyond usability. The accuracy here pertains to a marker of a certain geometry placed facing the camera-system.

In real-life scenarios, the marker is rarely if ever positioned face-on towards the camera. Thus, it is important to determine the rotational accuracy of a marker when it is detected by the camera in different orientations. To determine the rotational accuracy of a marker in different orientations, the marker geometry shown in Fig. 11 was rotated about the x-axis, a new marker geometry was defined from this orientation and the obtained marker was again analysed with *Atracsys Matlab Marker Analyzer*.

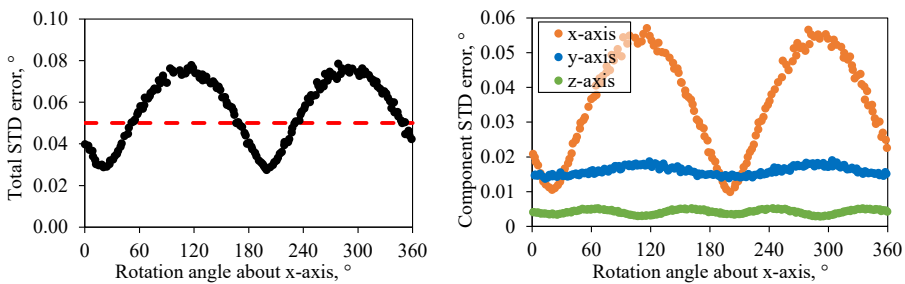


Fig. 11. **Left:** Rotational accuracy of a static marker as a function of rotation angle about the x-axis. The red line denotes the optimal maximum error of 0.05°. **Right:** The rotational accuracy of a static marker as a function of rotation angle about the x-axis separated into components.

As expected, rotating the marker decreases the accuracy with which it can be localized, as the area of the projection on the camera plane becomes smaller (Fig. 11 (left)). However, in Fig. 11 (right) it can

be seen that, even though most of the error is related to x-axis localization, rotating the marker about one axis introduces additional location errors for other axes as well.

## 4. CONCLUSIONS

---

For the investigation, *Atracsys fusionTrack 500* unit for optical pose tracking was used. Initial tests were also performed with the *Atracsys spryTrack 300*; however, the tracking accuracy of *Atracsys fusionTrack 500* was superior. Thus, it was the unit chosen for further measurements and as the base instrument for synthetic data constraints. Two types of IR diodes were tested as active markers – the SFH 4053 and SFH 4250-S – both produced by Osram. The SFH 4250-S was found to be more energy-efficient and slightly better in terms of fiducial localization accuracy. However, the SFH 4250-S has a larger package and consumes more power overall, while the improvement in localization accuracy is marginal.

To obtain the best possible angular accuracy when locating a marker, the area enclosed by the fiducials should be maximized. This, however, is limited by the available surface area of the HMD and occlusion also becomes an issue. Passive

markers can easily be placed on antennae-like protrusions; however, this is more difficult with active markers and the rigidity of the system can be challenging to achieve (and often adds unwanted weight to the HMD). A possible solution would be the creation of multi-face markers or the use of multiple markers for the localization of the HMD. However, the available space is still limited by the physical size of the HMD. Alternatively, a multi-camera set-up for high precision applications could be considered, but is likely to be relatively expensive.

In the experiments described above, the LEDs were driven continuously and, due to the comparatively low efficiency of IR LEDs, the heating of an HMD with a large number of fiducials might be unpleasant for the user. This could potentially be mitigated by pulsing the LEDs; however, this requires additional efforts from the software side as not to lose accuracy.

## ACKNOWLEDGEMENTS

---

The research has been supported by the Competence Centre of Electrical and Optical Equipment Production Sector of Latvia, project No. 1.2.1.1/18/A/006, study No. 1.16 “Development of an Integrated Elec-

tronic Solution for Determining the Position of the Head Display in the Room and Providing Remote Assistance Functionality”.

## REFERENCES

---

1. Khor, W. S., Baker, B., Amin, K., Chan, A., Patel, K., & Wong, J. (2016). Augmented and Virtual Reality in Surgery—The Digital Surgical Environment: Applications, Limitations and Legal Pitfalls. *Annals of Translational Medicine*, 4 (23), 454–454. <https://doi.org/10.21037/atm.2016.12.23>
2. Mekni, M., & Lemieux, A. (2014). Augmented reality: Applications, challenges and future trends. In: *Proceedings of the 13th International Conference on Applied Computer and Applied Computational Science (ACACOS'14)*, (pp. 205–214). 23–25 April 2014, Kuala Lumpur, Malaysia.
3. Fida, B., Cutolo, F., di Franco, G., Ferrari, M., & Ferrari, V. (2018). Augmented Reality in Open Surgery. *Updates in Surgery*, 70 (3), 389–400. <https://doi.org/10.1007/s13304-018-0567-8>
4. de Cunsel, S. (2019). Evaluation of Augmented Reality (AR) Displays Performance Based on Human Visual Perception. *Digital Optical Technologies*, 110620V. <https://doi.org/10.1117/12.2527613>
5. Tang, B., & Cao, S. (2020). A Review of VSLAM Technology Applied in Augmented Reality. *IOP Conference Series: Materials Science and Engineering*, 782 (4). <https://doi.org/10.1088/1757-899X/782/4/042014>
6. Ahn, J., Choi, H., Hong, J., & Hong, J. (2019). Tracking Accuracy of a Stereo Camera-Based Augmented Reality Navigation System for Orthognathic Surgery. *Journal of Oral and Maxillofacial Surgery*, 77 (5), 1070.e1-1070.e11. <https://doi.org/10.1016/j.joms.2018.12.032>
7. Welch, G., & Foxlin, E. (2002). Motion Tracking: No Silver Bullet, but a Respectable Arsenal. *IEEE Computer Graphics and Applications*, 22 (6), 24–38. <https://doi.org/10.1109/MCG.2002.1046626>
8. Nishino, H. (2010). A 6DoF fiducial tracking method based on topological region adjacency and angle information for tangible interaction. In: *Proceedings of the 4th International Conference on Tangible, Embedded, and Embodied Interaction – TEI '10* (vol. 18, p. 253). New York, New York, USA: ACM Press. <https://doi.org/10.1145/1709886.1709937>
9. Furtado, J. S., Liu, H. H. T., Lai, G., Lacheray, H., & Desouza-Coelho, J. (2019). Comparative Analysis of OptiTrack Motion Capture Systems. *Lecture Notes in Mechanical Engineering*, 15–31. [https://doi.org/10.1007/978-3-030-17369-2\\_2](https://doi.org/10.1007/978-3-030-17369-2_2)
10. Belghit, H., Bellarbi, A., Zenati, N., & Otmane, S. (2018). Vision-based Pose Estimation for Augmented Reality: A Comparison Study. *ArXiv*, 49413387.
11. Cutolo, F., Mamone, V., Carbonaro, N., Ferrari, V., & Tognetti, A. (2020). Ambiguity-Free Optical-Inertial Tracking for Augmented Reality Headsets. *Sensors (Switzerland)*, 20 (5). <https://doi.org/10.3390/s20051444>
12. Sorriento, A., Porfido, M. B., Mazzoleni, S., Calvosa, G., Tenucci, M., Ciuti, G., & Dario, P. (2020). Optical and Electromagnetic Tracking Systems for Biomedical Applications: A Critical Review on Potentialities and Limitations. *IEEE Reviews in Biomedical Engineering*, 13 (c), 212–232. <https://doi.org/10.1109/RBME.2019.2939091>
13. Bi, S., Gu, Y., Zou, J., Wang, L., Zhai, C., & Gong, M. (2021). High Precision Optical Tracking System Based on near Infrared Trinocular Stereo Vision. *Sensors*, 21 (7), 2528. <https://doi.org/10.3390/s21072528>
14. Ballestin, G., Solari, F., & Chessa, M. (2018). Perception and action in peripersonal space: A comparison between video and optical see-through augmented reality devices. In *2018 IEEE International Symposium on Mixed and Augmented Reality Adjunct (ISMAR-Adjunct)* (pp. 184–189). 16–20 October 2018, Munich, Germany. <https://doi.org/10.1109/ISMAR-Adjunct.2018.00063>

15. Javaid, M., & Haleem, A. (2020). Virtual Reality Applications toward Medical Field. *Clinical Epidemiology and Global Health*, 8 (2), 600–605. <https://doi.org/10.1016/j.cegh.2019.12.010>
16. Zabels, R., Osmanis, K., Narels, M., Smukulis, R., & Osmanis, I. (2019). Integrated Head-Mounted Display System Based on a Multi-Planar Architecture, *Advances in Display Technologies IX*, 10942, 51–61. <https://doi.org/10.1117/12.2509954>
17. Hai-Xia, X., Wei, Z., & Jiang, Z. (2015). 3D visual SLAM with a Time-of-Flight camera. In *2015 IEEE Workshop on Signal Processing Systems (SiPS)* (pp. 1–6). 14–16 October 2015, Hangzhou, China. <https://doi.org/10.1109/SiPS.2015.7344992>
18. Kunz, C., Maurer, P., Kees, F., Henrich, P., Marzi, C., Hlaváč, M., ... & Mathis-Ullrich, F. (2020). Infrared Marker Tracking with the HoloLens for Neurosurgical Interventions. *Current Directions in Biomedical Engineering*, 6 (1), 1–4. <https://doi.org/10.1515/cdbme-2020-0027>
19. Pérez-Pachón, L., Poyade, M., Lowe, T., & Gröning, F. (2020). Image Overlay Surgery Based on Augmented Reality: A Systematic Review. *Advances in Experimental Medicine and Biology*, 1260, 175–195. [https://doi.org/10.1007/978-3-030-47483-6\\_10](https://doi.org/10.1007/978-3-030-47483-6_10)
20. Atracsys. (2017). Data Sheet: fusionTrack 500. Available at <https://www.atracsys-measurement.com/wp-content/documents/FTk500-datasheet.pdf>
21. Khaleghi, B., & Rosing, T. Š. (2019). Thermal-Aware Design and Flow for FPGA Performance Improvement. *Proceedings of the 2019 Design, Automation and Test in Europe Conference and Exhibition, DATE 2019*, 342–347. <https://doi.org/10.23919/DATE.2019.8715183>
22. Israel, P. A. J., Carlos, P. O. J., Jorge, Á. S., Saúl, T. A., Emilio, V. S. J., & Susana, V. H. (2014). Design and construction of tools with reflecting-disks fiducials for optical stereo trackers: An affordable technique for navigation tools development. In: *11th International Conference on Electrical Engineering, Computing Science and Automatic Control, CCE 2014*, 5684680. 29 September–3 October 2014, Ciudad del Carmen, Mexico. <https://doi.org/10.1109/ICEEE.2014.6978258>